

Quantum tunnelling and hopping between metallic domains in disordered two-dimensional mesoscopic electron systems

This article has been downloaded from IOPscience. Please scroll down to see the full text article.

2009 J. Phys. A: Math. Theor. 42 214012

(<http://iopscience.iop.org/1751-8121/42/21/214012>)

View [the table of contents for this issue](#), or go to the [journal homepage](#) for more

Download details:

IP Address: 171.66.16.154

The article was downloaded on 03/06/2010 at 07:48

Please note that [terms and conditions apply](#).

Quantum tunnelling and hopping between metallic domains in disordered two-dimensional mesoscopic electron systems

D Neilson^{1,2} and A R Hamilton³

¹ Dipartimento di Fisica, Università di Camerino, I-62032 Camerino, Italy

² NEST CNR-INFM, I-56126 Pisa, Italy

³ School of Physics, University of New South Wales, Sydney 2052, Australia

E-mail: david.neilson@unicam.it

Received 2 November 2008, in final form 17 January 2009

Published 8 May 2009

Online at stacks.iop.org/JPhysA/42/214012

Abstract

We investigate transport in 2D mesoscopic electron systems with disorder assuming a percolation mechanism through a network of disconnected conducting metallic domains. The size of the domains is determined by the level of disorder and the strength of the electron correlations. The domains are linked for transport by two competing mechanisms. The first mechanism is familiar thermally activated hopping. The second is quantum tunnelling between adjacent conducting regions bounded by equipotential contours of the same value. This mechanism leads to temperature-independent transmission at low temperatures. We calculate the transmission across the potential barriers separating adjacent domains, and we obtain agreement with recent experimental measurements of temperature-dependent resistivities in mesoscopic 2D systems. We also obtain consistent values for the spatial separation of the domains and the average variation in the random disorder potential. Finally, we show that the effect of quantum coherence can result in a small downturn in the resistivity at low temperatures, again in good agreement with the recent experimental results.

PACS numbers: 73.20.Dx, 71.30.+h, 73.40.-c

(Some figures in this article are in colour only in the electronic version)

The interplay between electron correlations and disorder plays a central role in determining the transport properties of dilute two-dimensional (2D) electron systems [1]. The nature of the ground state of these systems is determined by competition between the random potential fluctuations from disorder and the interactions between the electrons.

In modulation-doped GaAs/AlGaAs heterojunctions, the main source of disorder comes from the remote charged ions in the doping layer. The strength of the disorder depends

sensitively on the width δ of the undoped spacer layer separating the 2D electron system from the dopants. Typical values of δ are ~ 50 nm. Imaging of the disorder in these systems suggests the dominant disorder length scale in modulation-doped GaAs/AlGaAs heterostructures is greater than $0.5 \mu\text{m}$ and hence much greater than δ [2, 3]. These experimental data indicate that long-range disorder dominates on a macroscopic length scale. In the very high mobility 2D electron layers in undoped GaAs/AlGaAs heterojunctions [4] the electron layer is field induced. However, even in the absence of a doping layer it is believed that long-range disorder dominates due to randomly distributed residual charged impurities, and very recent studies of undoped mesoscopic structures show signatures of background disorder [5].

For disorder that is mainly long range, the system can be expected to become increasingly inhomogeneous at low electron densities, and the random potential fluctuations may create a percolative second-order transition in the transport coefficients. The potential fluctuations could create domains consisting of regions of lower and higher density [4, 6]. As the average electron density is decreased this can lead to a classical insulator to metal transition [7].

Experimental evidence for localized domains has been found in gated GaAs heterostructures using near field spectroscopy with sub-wavelength resolution [8]. Negatively charged exciton luminescence is used to image the spatial distribution of the electrons in a 2D layer. In the range of gate voltages where the conductivity drops, the electrons have been shown to be localized inside the potential fluctuations of the remote ionized donors. The spectral signature of regions filled with localized electrons was very different from regions containing conducting electrons. Similar evidence of spatial inhomogeneities at low carrier densities has been observed in scanning probe measurements [9].

If long-range disorder is strong and dominant, then transport will obey classical percolation theory, and the interactions between electrons will be a secondary effect [4]. In order to separate out the effect of short-range fluctuations from disorder, Baenninger *et al* [10] have recently compared transport in large-area macroscopic and narrow mesoscopic 2D electron systems in modulation-doped GaAs/AlGaAs gated structures. In the large-area macroscopic samples, transport is determined by the large long-range fluctuations, and the expected insulating behaviour was observed for the range of electron densities studied. However, the lengths of the mesoscopic devices, $\sim 1 \mu\text{m}$, are smaller or comparable to the length scale of long-range disorder, so that the long-range disorder potential is practically constant across the mesoscopic systems (figure 1). This permits residual short-range fluctuations of the random impurity potential to dominate transport properties for these systems.

For the experiments in [10] a metal top gate was used to tune the electron density across a range which was always well inside the insulating phase. The electrons were degenerate, with Fermi temperatures $4 \lesssim T_F \lesssim 7$ K. Down to temperatures $T \sim 1$ K, the resistivity $\rho(T)$ was observed to follow the familiar insulator-like activated temperature dependence, but for temperatures lower than a crossover temperature $T_\theta \sim 1$ K the behaviour of $\rho(T)$ changed dramatically. It either saturated (see, for example, the experimental data points from [10] in figure 2(a)), or else there was a turn-over and $\rho(T)$ actually decreased slightly when T was further decreased (see, for example, the data points in figure 2(b)). This crossover behaviour occurred for resistivities as high as $\rho \sim 400 \hbar/e^2$, and was observed over two orders of magnitude in the resistivity.

Here we discuss theoretical evidence that both the saturation and the turn-over of $\rho(T)$ at low T are due to quantum effects associated with tunnelling between states of the same energy in adjacent disconnected conducting regions in the insulating phase.

This might seem at first sight surprising since it occurs so deep in the insulating regime but we shall see that it is not inconsistent with Mott's original concept of variable range hopping [11]. The length scale and strength of the variations of the random impurity potential in the

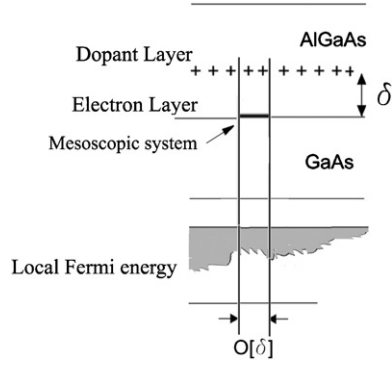


Figure 1. δ is the width of the undoped spacer layer separating a 2D electron system from the layer of dopants in modulation-doped GaAs/AlGaAs heterojunction. For a mesoscopic system shorter than length scale of long-range disorder, it is the short-range fluctuations of the random impurity potential of $\mathcal{O}[\delta]$ that will dominate.

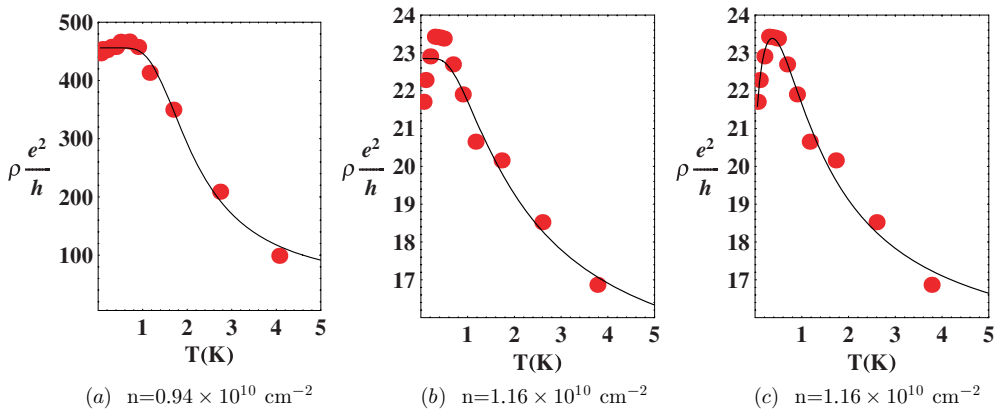


Figure 2. Points are measured resistivity ρ as a function of T at fixed electron densities n taken from figure 2 of [10]. (Points in (b) and (c) are the same.) Curves in (a) and (b) are calculated using equation (6). For the curve in (c) we used equation (9).

mesoscopic samples of [10] are much smaller than in their macroscopic samples, and we propose that this significantly increases the effect of quantum tunnelling rates between states of the same energy.

We start with a 2D system in the insulating regime which is a composite of an insulating phase I and a metallic (conducting) phase M (figure 3(a)). We assume at an insulator–metal transition at critical density n_c the ground state energies $E_I(n)$ and $E_M(n)$ cross. We initially assume the random potential $V_{\text{imp}}(\mathbf{r})$ associated with the impurities varies smoothly, in the sense that its fluctuation length scale ℓ_v exceeds the correlation length of the metallic phase ξ_M . The local energy density is then given by $E(\mu - V_{\text{imp}}(\mathbf{r}))$, with μ being the chemical potential.

The impurity potential $V_{\text{imp}}(\mathbf{r})$ breaks the system into domains approximately bounded by equipotential contours $V_{\text{imp}}(\mathbf{r}) = \mu_c$ where μ_c is the chemical potential at the density n_c . This leads to spatial inhomogeneities in the local electron density. Such a domain model has been employed by Shimshoni *et al* [12] to study transport properties near the phase transition

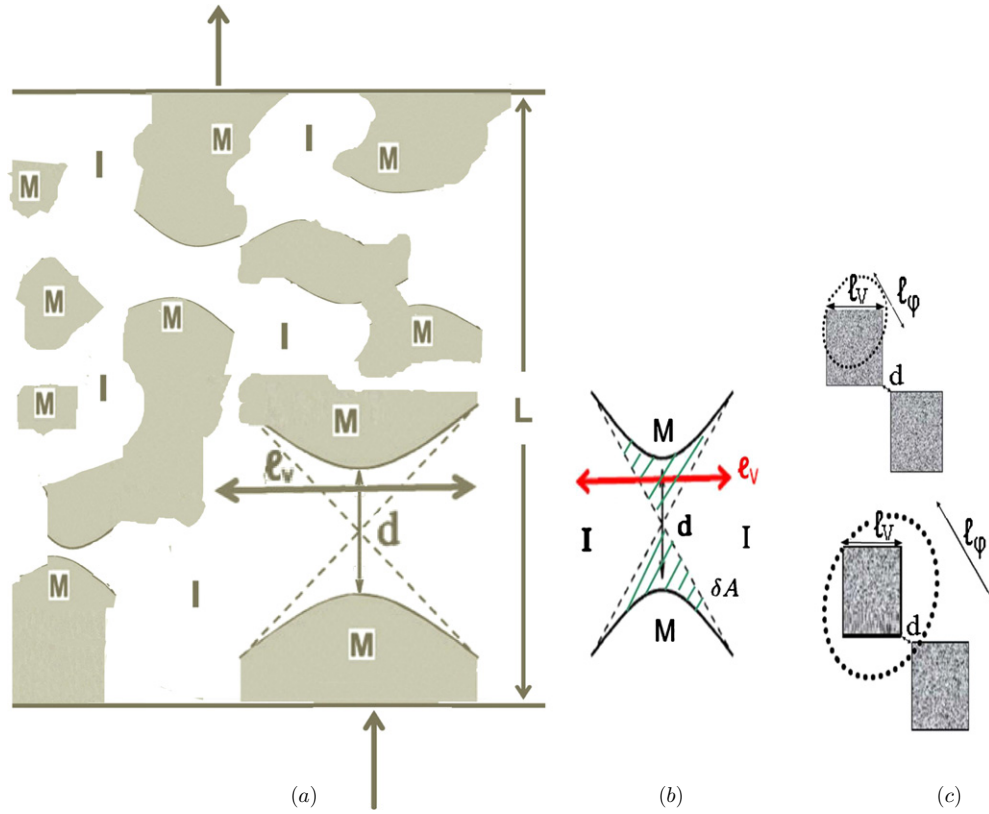


Figure 3. (a) Arrows indicate the direction of transport across short ($L \sim 0.5\text{--}2 \mu\text{m}$) mesoscopic 2D electron insulating state. With disorder, the insulating system can break up into a composite of insulating I (light) and metallic M (shaded) domains. (b) At boundaries of adjacent metallic domains (solid lines) $V_{\text{imp}}(\mathbf{r})$ is a constant μ_c . The metallic domains are separated by a distance d . Hatched region δA is the excess area of the insulating domain for the junction. ℓ_v is the fluctuation length scale of $V_{\text{imp}}(\mathbf{r})$. (c) Upper panel: at higher T , the phase coherence length ℓ_ϕ is shorter than average dimensions of the metallic regions, ℓ_v , and only incoherent propagation across each metallic region contributes. Lower panel: at low T the length ℓ_ϕ becomes comparable to ℓ_v , and coherent propagation across two metallic regions becomes possible.

for quantum Hall insulators and superconductors. Meir [13] and Neilson *et al* [14] have used the domains model to study transport around the 2D metal–insulator transition, with the domains consisting of coexisting metal and insulating phases. The metallic domains will form in regions of higher electron density $V_{\text{imp}}(\mathbf{r}) < \mu_c$, with the insulating domains occupying the remaining areas.

In the domains model for 2D systems, the percolation threshold occurs when the total areas of the two types of domains are equal, so the critical insulator area fraction is $p = \frac{1}{2}$. For this unique value of p , both the insulating and metallic domains contain at least one connected path across the sample, and all neighbouring domains will touch just at one point. $V_{\text{imp}}(\mathbf{r})$ must form a saddle point centred on the contact point since it increases from the contact point as we move into the adjacent metallic domains (lower electron density) but decreases as we move into the adjacent insulating domains (higher electron density).

As the average electron density n is decreased away from the percolation threshold, the metallic phase retreats from the centre of the junction and is replaced by the insulating phase.

The dotted lines in figures 3(a) and (b) mark the domain boundaries at the transition where the area fraction was exactly equal to $p = \frac{1}{2}$. Thus the area of the insulating phase at the junction for all $p > 1/2$ will exceed the area of the metallic phase by δA . This is the area enclosed by the metallic boundaries and the dotted lines. Assuming a hyperbolic form for each metallic boundary near the junction it is straightforward to show [12]

$$\delta A = (1/2) \log(\ell_V/d)d^2, \quad (1)$$

where d is the minimum distance separating adjacent metallic phase domains and is a function of electron density. ℓ_V is the fluctuation length scale of the random impurity potential, which we assume is large compared with d .

Mott's original concept of variable range hopping describes the behaviour of the resistivity in strongly disordered systems with hopping between localized states centred on fixed sites. There is competition between the overlap term for two localized regions and the energy activation. The overlap term favours short hops, while energy activation favours long hops since long hops will provide more opportunity to reduce the activation energy. As the temperature is decreased the range of activation energies becomes ever more restricted, and this favours the longer hops. As the average hops become longer, the optimized overlaps decrease, leading to the familiar result of a resistivity that increases exponentially with decreasing temperature.

In the domains model, the same variable range hopping mechanism acts at higher temperatures, but at low enough temperatures the transmission will be dominated by tunnelling between adjacent metallic regions, with both regions bounded by equipotential contours of the same value (figure 3(b)). This transmission is independent of temperature and is given by the zero-temperature tunnelling rate.

In the domains model, we determine the resistivity from the transmission across the quantum junctions as a function of d since the primary contribution to the resistivity comes from the saddle point of the potential near $V_{\text{imp}}(r) \sim \mu_c$. We initially assume that quantum interference effects take place only on a length scale small compared with ℓ_V so there is no coherence between tunnelling events. For a finite width distribution of junction resistances in a two-dimensional array, the total resistance is given by the resistance of the most resistive junction, the so-called 'worst resistance' [13, 15]. The resistivity depends on the temperature-dependent transmission rate $\mathcal{T}(T)$ through this junction, $\rho(T) = (1 - \mathcal{T}(T))/\mathcal{T}(T)$ in units of \hbar/e^2 .

Since at relatively high temperatures the transport across the junction is by thermally activated hopping, the transmission is

$$\begin{aligned} \mathcal{T}_{\text{th}} &\sim \int_{V_{\text{barr}}}^{\infty} \exp(-E/k_B T) dE \\ &= \mathcal{T}_0 \exp\left(-\frac{V_{\text{barr}}}{k_B T}\right). \end{aligned} \quad (2)$$

The constant \mathcal{T}_0 is the transmission for $d = 0$, that is at the percolation threshold. V_{barr} is the barrier height across the junction. It is related to V'' , the curvature of the impurity potential at the junction, by $V_{\text{barr}} = (1/2)V''(d/2)^2$.

The zero-temperature tunnelling transmission through the barrier is given by

$$\mathcal{T}_{\text{tun}}(0) \sim \exp(-2S(d)) = \mathcal{T}_0 \exp(-S''d^2), \quad (3)$$

where the action across the barrier is $S(d) \simeq S(0) + \frac{1}{2}S''d^2$. The second derivative of the action can be expressed as $S'' = (\pi/2\hbar)\sqrt{mV''}$, so equation (3) can be written as

$$\begin{aligned} \mathcal{T}_{\text{tun}}(0) &= \mathcal{T}_0 \exp(-(\pi/2\hbar)\sqrt{mV''}d^2) \\ &= \mathcal{T}_0 \exp(-(\pi/\hbar)\sqrt{2mV_{\text{barr}}}d). \end{aligned} \quad (4)$$

From equations (2) and (4) the resistivity can be written in two limits as

$$\rho(T, n) = \mathcal{T}_0^{-1} \exp \left[\frac{\pi \sqrt{2mV_{\text{barr}}} d}{\hbar} \right] - 1; \quad T = 0 \quad (5a)$$

$$= \mathcal{T}_0^{-1} \exp \left[\frac{V_{\text{barr}}}{k_B T} \right] - 1; \quad \text{large } T. \quad (5b)$$

Equation (5) gives the limiting behaviours of the resistivity. The resistivity increases exponentially with decreasing temperature at higher temperatures but it goes to a finite low-temperature value because of quantum tunnelling between states of the same energy in adjacent metallic domains.

Interpolating between these contributions, we can write

$$\rho(T, n)^{-1} = \mathcal{T}_0 \exp \left[-\frac{\pi \sqrt{2mV_{\text{barr}}} d}{\hbar} \right] + \mathcal{T}_0 \exp \left[-\frac{V_{\text{barr}}}{k_B T} \right] - 1. \quad (6)$$

We used equation (6) to fit measured temperature-dependent resistivity data from figure 2 in [10]. The solid lines in figures 2(a) and (b) show the fits of equation (6) to the experimental points. For electron density $n = 0.94 \times 10^{10} \text{ cm}^{-2}$ the fitting parameters were $V_{\text{barr}} = 0.5 \text{ meV}$, $d = 5 \text{ nm}$, $\mathcal{T}_0 = 0.03 \text{ s}^{-1}$, and for $n = 1.16 \times 10^{10} \text{ cm}^{-2}$, $V_{\text{barr}} = 0.2 \text{ meV}$, $d = 2 \text{ nm}$, $\mathcal{T}_0 = 0.03 \text{ s}^{-1}$. We conclude that equation (6) reproduces the features of the experimental data very well, with the exception of the turn-down in the measured resistance for $T \lesssim 1 \text{ K}$ in figure 2(b).

We now investigate the cause of this drop in resistance. We note that it is a relatively small effect, $\lesssim 10\%$ of the total resistance. It is clear that our model of a single junction, which we have demonstrated, leads to a saturation of the resistance, cannot cause an actual drop in resistance. Therefore we must generalize the model.

Up to this point we have assumed that the characteristic size of the conducting regions is sufficiently large that the electrons always have time to decohere between tunnelling events. However, this assumption must start to break down for sufficiently small T since the coherence length, the characteristic scale for coherent propagation, is inversely proportional to temperature: $\ell_\phi = (\hbar k_F D)/(\pi T) = \hbar^2 k_F^2 \ell / (2\pi m k_B T) = (T_F/T)(\ell/\pi)$, where ℓ is the mean free path for elastic scattering.

We estimate at electron densities for which $T_F \sim 5 \text{ K}$ that ℓ_ϕ becomes comparable to ℓ around $T \sim 1 \text{ K}$. We can assume $\ell \lesssim \ell_v$. As ℓ_ϕ approaches ℓ_v from above, coherent propagation across the metallic regions bounding the highest resistance junction becomes increasingly likely (see figure 3(c)). In this case, the total transmission is the sum of the incoherent transmission $\mathcal{T}_{\text{incoh}}$ plus a small contribution from coherent transmission \mathcal{T}_{coh} ,

$$\tilde{\mathcal{T}}_{\text{tun}} = \mathcal{T}_{\text{incoh}} + \mathcal{T}_{\text{coh}}. \quad (7)$$

\mathcal{T}_{coh} becomes increasingly significant as the temperature is further decreased.

Since we are deep in the insulating region, we can expect the transmission probabilities across the junction to be small. Then we can write equation (7) as [16]

$$\tilde{\mathcal{T}}_{\text{tun}} = \mathcal{T}_{\text{incoh}} [1 - (1 - \epsilon(T)) \cos \Phi]. \quad (8)$$

The probability that an electron traverses the conducting region without scattering, $1 - \epsilon \sim \exp(-\ell_v/\ell_\phi)$, is temperature dependent because of ℓ_ϕ , $1 - \epsilon(T) \sim \exp((-\ell_v/\ell)(\pi T/T_F))$. The phase Φ is the total phase change of the electron in its coherent transmission across the conducting region and the junctions.

Generalizing equation (6) using equation (8), we can write the contribution to the temperature-dependent resistivity from the combined effect of thermal hopping and tunnelling as

$$\rho(T, n)^{-1} = \mathcal{T}_0 \exp \left[-\frac{\pi \sqrt{2m V_{\text{barr}}} d}{\hbar} \right] \left[1 - \exp \left[\left(-\frac{\ell_v}{\ell} \right) \left(\frac{\pi T}{T_F} \right) \right] \cos \Phi \right] + \mathcal{T}_0 \exp \left[-\frac{V_{\text{barr}}}{k_B T} \right] - 1. \quad (9)$$

We used equation (9) to fit the resistivity data from figure 2 in [10] for electron density $n = 1.16 \times 10^{10} \text{ cm}^{-2}$. The solid line in figure 2(c) shows the excellent fit to the experimental points we obtain using equation (9). This now includes the turn-down in the resistivity at low T . Since the coherence effect remains a small correction down to the lowest temperatures in the experimental data, ~ 50 mK, we only needed to fit the additional parameters, the ratio (ℓ_v/ℓ) and the phase Φ , leaving V_{barr} , d and \mathcal{T}_0 unchanged from figure 2(b). The values in figure 2(c) are $(\ell_v/\ell) = 14$ and $\cos \Phi = -0.1$.

The potential barriers, $V_{\text{barr}} \sim 0.2\text{--}0.5$ meV, are much smaller than the variations $\Delta V_{\text{disorder}} \sim 2\text{--}5$ meV measured in macroscopic samples by Finkelstein *et al* [2] and Chakraborty *et al* [3]. The values of the length scale of the disorder variation reported in [2, 3] are also much greater than our values for d . This is consistent with the suggestion that in the mesoscopic samples of [10] it is short-range fluctuations of $\mathcal{O}(\delta)$ that dominate.

In conclusion, we have applied a model for the insulating phase of the 2D electron system in which there are domains of metallic and insulating regions caused by the random fluctuations of the impurity potential. This leads to calculated resistivities with properties that are in agreement with recent measurements of the temperature-dependent resistivity in mesoscopic samples. The analysis requires only that the insulating component is sufficiently insulating for transport to be dominated by a path that avoids the insulating component as much as possible. Thus the model can apply well into the insulating regime, with resistances as large as $\rho \sim 400(e^2/h)$. The observed crossover to a saturation of the temperature-dependent resistivity for $T \lesssim 1$ K is understood as the effect of quantum tunnelling between states of equal energy. This is due to the boundaries of the adjacent metallic regions having equipotential contours of the same value and leads to a transmission that is independent of temperature. We associate the small turn-down in the resistivity which sometimes occurs with the increase in the quantum coherence length as the temperature is lowered.

The reason in the mesoscopic systems that the effects are observed at temperatures as high as $T \sim 1$ K is that the weaker variations of the random impurity potential lead to lower potential barriers V_{barr} between the adjacent metallic regions than is the case for the corresponding macroscopic systems. In addition, the shorter-range nature of the random impurity potential reduces the separations d between adjacent metallic regions. These decreases in V_{barr} and d favour tunnelling between equal energy states of neighbouring metallic regions.

Acknowledgment

We thank Arindam Ghosh for useful discussions.

References

- [1] Simonian D, Kravchenko S V, Sarachik M P and Pudalov V M 1997 *Phys. Rev. Lett.* **79** 2304
- [2] Finkelstein G, Glicofridis P I, Ashoori R C and Shayegan M 2000 *Science* **289** 90
- [3] Chakraborty S, Maasilta I J, Tessmer S H and Melloch M R 2004 *Phys. Rev. B* **69** 073308
- [4] Das Sarma S, Lilly M P, Hwang E H, Pfeiffer L N, West K W and Reno J L 2005 *Phys. Rev. Lett.* **94** 136401
- [5] Sarkozy S, Das Gupta K, Siegert C, Ghosh A, Pepper M, Farrer I, Beere H E, Ritchie D A and Jones G A C 2009 *Appl. Phys. Lett.* **94** at press (arXiv:0807.2778v1)
- [6] Efros A L 1989 *Solid State Commun.* **70** 253

- Davies J H, Nixon J A and Baranger H U (unpublished)
Shklovskii B I and Efros A L 1984 *Electronic Properties of Doped Semiconductors* (Berlin: Springer)
- [7] Nixon J A and Davies J H 1990 *Phys. Rev. B* **41** 7929
 - [8] Eytan G, Yayan Y, Rappaport M, Shtrikman H and Bar-Joseph I 1999 *Phys. Rev. Lett.* **81** 1666
 - [9] Ilani S, Yacoby A, Mahalu D and Shtrikman Hadas 2000 *Phys. Rev. Lett.* **84** 3133
 - [10] Baenninger M, Ghosh A, Pepper M, Beere H E, Farrer I and Ritchie D A 2008 *Phys. Rev. Lett.* **100** 016805
 - [11] Mott N F 1969 *Phil. Mag.* **19** 835
 - [12] Shimshoni E, Auerbach A and Kapitulnik A 1998 *Phys. Rev. Lett.* **80** 3352
 - [13] Meir Y 2000 *Phys. Rev. B* **61** 16470
 - [14] Neilson D, Thakur J S and Tosatti E 2000 *Aust. J. Phys.* **53** 531
 - [15] Shimshoni E and Auerbach A 1997 *Phys. Rev. B* **58** 9817
 - [16] Büttiker M 1988 *IBM J. Res. Dev.* **32** 63